HIGH-RESOLUTION NUMERICAL MODELLING OF STRESS-STRAIN FIELDS IN THE VICINITY OF A CRACK TIP SUBJECTED TO FATIGUE

J. Toribio and V. Kharin*

Finite deformation analysis of the cracked elastoplastic panel with a plane-strain crack subjected to mode I (opening) cyclic loading under small scale yielding was performed to elucidate the influence of the load range, load ratio and overload peak on the crack-tip shape and near-tip stress and strain fields. At zero-to-tension constant amplitude loading no evidence of geometric crack closure (contact of the crack faces) at load removals was detected, neither after a single overload peak. Cyclically stable evolution patterns of stress, plastic strain and strain energy density established near the crack tip after a couple of loading cycles.

INTRODUCTION

Fatigue of materials under alternating loads is the cause of many engineering failures, so that fatigue crack growth rate *da/dN* is the key issue in damage tolerant design (Suresh (1)). When inelastic material behaviour (plasticity, damage, etc.) is localised in a small near tip domain —the small scale yielding (SSY) case— the concepts of linear elastic fracture mechanics can be used and the stress intensity factor K is expected to work well. The basic fatigue law may be represented as:

$$\frac{da}{dN} = \mathcal{F}(K_{max},K_{min}) = \widetilde{\mathcal{F}}(\Delta K,R) \qquad (1)$$

where the right hand parts are material-dependent functions, K_{max} and K_{min} are, respectively, the maximum and minimum K-values of the loading cycle; $\Delta K = K_{max}-K_{min}$ the stress intensity range and $R = K_{min}/K_{max}$ the load ratio.

Micromechanisms of fatigue degradation and rupture are thought to be related to cyclic evolutions of stress and strain, ref. (1), whereas the K can be the controlling parameter but not a direct driver. Thus analyses of fine peculiarities of local crack tip stresses and strains are essential for linking controllable macroscopic

* Department of Materials Science, University of La Coruña, E.T.S.I. Caminos, Campus de Elviña, 15071 La Coruña, Spain.

variables such as K with fracture mechanisms. Theoretical models of the near tip situation under cyclic loading have been developed (Rice (2)), as well as numerical simulations under plane stress (cf. McClung et al. (3)) without accounting for a large deformations effect. Only the paper by Gortemaker et al. (4) offered limited data on large-strain elastoplastic crack tip situation for a single cycle "loading-unloading-reloading". Meanwhile, these matters deserve more attention because all the events relevant to the near tip rupture and crack advance take place in the intensively strained very-near tip zone where the situation along the crack front in the interior is closer to plain strain state.

BASIC MODELLING ISSUES

The model material is supposed to be rate-independent ideal elastoplastic with von Mises yield criterion. Its characteristics are chosen relevant to typical steels: Young modulus E = 200 GPa, Poisson ratio μ = 0.3, tensile yield stress σ_Y =600 MPa (nevertheless, the solutions are applicable to some similitude class of situations fixed by the ratio σ_Y/E and by the crack tip geometry, cf. McMeeking (5)). The crack has initially parallel flanks and smooth round-shape tip of a width (twice the tip radius) b_0, which seems to be a reasonable approximation (discussion can be found elsewhere (5), and experimental support in the paper by Handerhan and Garrison (6)). For medium-strength steels the value b_0 = 5 μm is used (6). The upper bound for applied K-values is limited to 60 MPam$^{1/2}$ which is appropriate for steels as a range at which fatigue cracking goes on. With these parameters the crack length is taken a = 75 mm to enforce the conditions of K-dominated SSY near the tip. The double-edge-cracked panel under remote tension by uniform stress σ_{app} is considered using K-solution from the compendium by Savruk (7) as follows:

$$K = 1.158\ \sigma_{app} \sqrt{\pi\ a} \qquad (2)$$

Computations were performed for several constant amplitude loading patterns at different amplitudes and load ratios. In addition, the effect of a single overload peak was considered. K was a control variable in this study, depending on which corresponding applied load levels σ_{app} were established according to relation (2). The following load cases were considered in the numerical simulations:

(I) K_{max} = 60 MPam$^{1/2}$, K_{min} = 0 (R = 0);
(II) K_{max} = 30 MPam$^{1/2}$, K_{min} = 0 (R = 0);
(III) K_{max} = 60 MPam$^{1/2}$, K_{min} = 30 (R = 0.5);
(IV) K_{max} = 30 MPam$^{1/2}$, K_{min} = 0 (R = 0), overload to K_{ov} = 60 MPam$^{1/2}$.

and up to ten loading cycles (twenty load reversals) were completed in each case. To avoid excessive distortion of the finite element mesh, thus permitting calculations for several load reversals, the near tip mesh required more refinement than in simulations at rising-only load (5). The load stepping procedure in the incremental elastoplastic solution had to be finer than those for small-strain cycling (3) and large-strain single cycle modelling (4). Several near-tip mesh refinements were tried, and the optimum one of 1148 four-node quadrilaterals with 1222 nodes was used. The solution of the boundary value problem was accomplished using the nonlinear finite element code MARC (8) with an updated Lagrangian formulation.

RESULTS

Near-tip crack profiles evolve with load cycling in a similar manner for all load cases. As an example, crack tip deformation corresponding to the load pattern I is depicted in Fig. 1. It should be noted that geometrical crack closure (contact of its faces) was never detected in performed simulations. Crack width at unloading to $K = 0$ always remained quite considerable, and it never and nowhere returned to the original width b_0. This agrees with previous work in ref. (4) but contradicts, however, the results of ref. (3).

Details on the stress state are given in Fig. 2 where the odd times $t = 2k - 1$ correspond to load maxima and the even ones $t = 2k$ to minima in the k-th cycle. Stress distributions beyond the tip at similar load cases I and II (the same $R = 0$) are nearly identical if displayed in terms of the distance X of the material point from the tip apex in the original configuration normalised by the current deformed crack tip width b. Stress fields are moderately sensitive to the load ratio and load sequence.

Stress evolutions beyond the tip in material points identified by their coordinates in the original configuration $X_1 = 279b_0 > X_2 = 18b_0 > X_3 = 1.7b_0$ under a sine-shape applied load history are given in Fig. 3. The stress histories far from the tip (point X_1) replicate fairly the sine-like alteration of the applied load. Near the crack tip after just about the first cycle the $\sigma_{yy}(t)$ acquires a stable cyclic regime as a repetition of nearly the same Π-like shape with stress ratio close to -1 different from the applied load ratio. This is common for all the load cases.

A certain affinity was found between evolutions of the near tip plastic strain ε_{yy}^p, equivalent plastic strain ε_{eq}^p, and strain energy density W. Fig. 4 displays the strain accumulation as a ratcheting elevation with alteration "amplitudes" for all load cases in apparent correspondence with their respective ΔK-values. The averaged slopes $\Delta\varepsilon_{yy}^p/\Delta N$ (secant lines from the origin) decrease from one load case to another in the sequence I $\rightarrow$ III $\rightarrow$ II $\rightarrow$ IV (extrapolated post-overload value).

DISCUSSION

To derive implications for fatigue crack growth, a crack advance criterion is required. From the performed simulations it follows that because of the observed mutual affinity of the averaged ratcheting (or "climbing") accumulation behaviours of the three candidates such as ε_{yy}^p, ε_{eq}^p and W, all them have equal opportunities to succeed in monitoring damage accumulation near the crack tip, and agreement can be noticed between them and known regularities of the observed fatigue response of materials in terms of crack growth rate. All of them decelerate from one load case to another following the same order I $\rightarrow$ III $\rightarrow$ II $\rightarrow$ IV (post-overload rate), see Fig. 4.

To establish a firm and general crack growth equation of the kind (1), a promising way seems to be joining of high-resolution stress-strain analysis with the concepts analogous to those used in micromechanical modelling of local fracture near the crack tip to estimate the critical K-value under monotonous loading on the basis of either critical strain ε_c, or critical absorbed energy density W_c. Owing to the mentioned parallelism between variation of experimental crack growth

rate and calculated effective rates of evolution of plastic strains and strain energy density near the crack tip under various loading conditions, this way towards developing predictive tools for fatigue crack growth seems to be promising.

CONCLUSIONS

High-resolution large deformation finite-element analysis of a stationary plane-strain tensile crack in ideal elastoplastic solid under various cyclic load patterns was performed. Geometrical crack closure was never detected.

The most notable peculiarities of the cyclic near-tip stress fields common for all simulated load cases are the following: (*a*) self-similitude of the spatial distribution of stresses; (*b*) attaining of the steady state regime of cyclic variation with Π-like shape different from the applied load pattern shapes.

Near tip patterns of plastic strain ε_{yy}^{p}, total equivalent plastic strain ε_{eq}^{p} or strain energy density W (this latter was found be strain-dominated) exhibit persistent ratcheting or climbing behaviours which may be characterised by certain values of average accumulation rates dependent on external load range, load ratio and overload peak. These calculated accumulation rates agree with experimentally observable trends of the influence of the external loading characteristics on fatigue crack growth rates.

Acknowledgement. This work was funded by the Spanish CICYT (Grant MAT97-0442) and Xunta de Galicia (Grants XUGA 11801B95 and XUGA 11802B97). One of the authors (VKh) is indebted to Xunta de Galicia and DGICYT (Grants SAB95-0122 and SAB95-0122P) for supporting his stays, respectively, as a visiting scientist and sabbatic professor at the University of La Coruña.

REFERENCES

(1) Suresh, S., "Fatigue of Materials", Cambridge University Press, Cambridge, UK, 1991.

(2) Rice, J.R., ASTM STP 415, 1967, pp. 247-309.

(3) McClung, R.C., Thacker, B.H. and Roy, S., Int. J. Fracture, Vol. 50, 1991, pp. 27-49.

(4) Gortemaker, P.C.M., de Pater, C. and Spiering, R.M.E.J., Proceddings of the 5th Int. Conf. Fracture. Edited by D. Francois, Pergamon Press, Oxford, 1981, pp. 151-160.

(5) McMeeking, R.M., J. Mech. Phys. Solids, Vol. 25, 1977, pp. 357-381.

(6) Handerhan, K.J. and Garrison, W.M., Jr., Acta Metall. Mater., Vol. 40, 1992, pp. 1337-1355.

(7) Savruk, M.P., "Stress Intensity Factors in Solids With Cracks", Naukova Dumka, Kiev, 1988 (in Russian).

(8) MARC User Information, Marc Analysis Research Corp., Palo Alto, 1994.

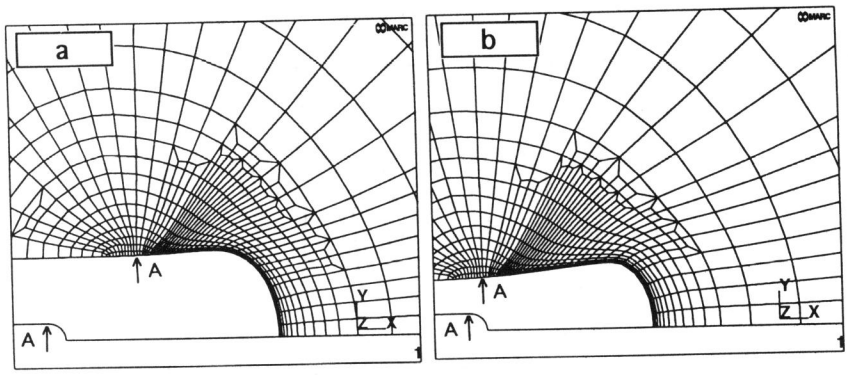

Figure 1. Near-tip deformations at different stages of load case I: (a) at the 4th maximum load point, $K = K_{max}$; (b) at subsequent unloading point, $K = 0$ (the original crack tip is shown in the bottom left corners).

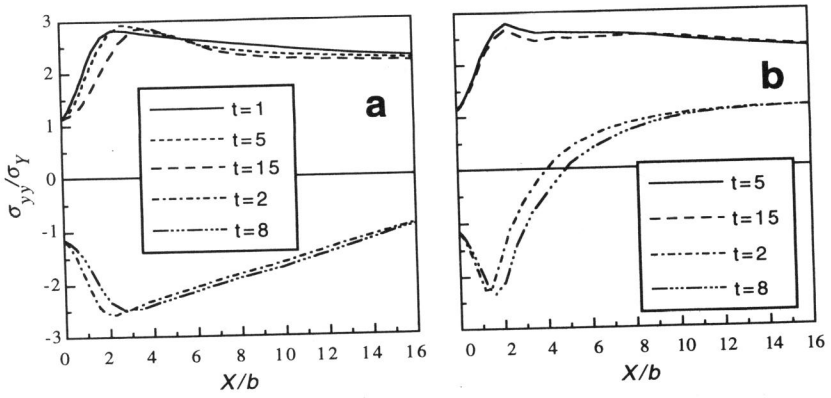

Figure 2. Normal stress σ_{yy} near the crack tip : (a) load case I; (b) load case III.

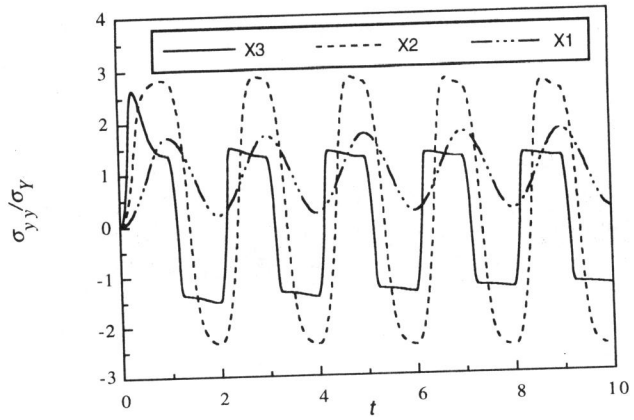

Figure 3. Evolution of the normal stress σ_{yy} in the points $X_{1,2,3}$ beyond the crack tip at sine-shape applied load pattern (load case I).

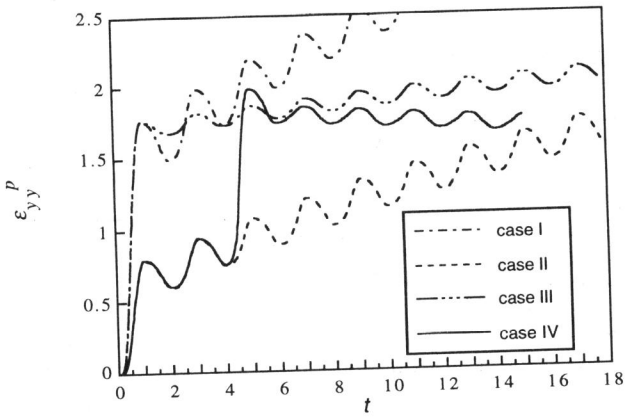

Figure 4. Plastic strain evolutions in the crack tip (overload peak in the load case IV occurs at $t = 5$).